# JMEMS Letters

## Direct Growth and Fabrication of Tungsten Coated GaN Nanowire Probes on Cantilevers for Scanning Probe Microscopy

Kristen L. Genter, Matt D. Brubaker, Samuel Berweger, Jonas C. Gertsch, Kris A. Bertness, Pavel Kabos, and Victor M. Bright, *Fellow, IEEE*

***Abstract*— Gallium nitride nanowires (NWs) grown on silicon-on-insulator wafers by means of selective area epitaxy are directly integrated into scanning probe cantilever fabrication. These cantilevers with NW probe tips are coated with tungsten by atomic layer deposition to take measurements on gold embedded in silicon to test the RF response of the cantilever to changes in the material properties. The sensitivity of the cantilever RF capacitance measurement was tested on a microcapacitor reference sample with 0.7 – 7.1 $\mu m^2$ microcapacitors on 10 $nm$ $SiO_2$ steps. These probes have an estimated noise-limited sensitivity of 12.5 $aF$, demonstrating the first RF cantilever with a selectively grown NW probe tip. [2021-0240]**

***Index Terms*— Atomic layer deposition, gallium nitride, nanowires, scanning microwave microscopy, tungsten, scanning microwave impedance microscopy.**

### I. Introduction

THE importance of repeatable characterization of advanced material properties on the micro- and nanoscales has been a driver in the advancement of scanning probe technologies. Central components of scanning probe instruments to obtain these enhanced measurements are the dimensions of the probe and the probe's material properties. For this reason, research has been focused on utilizing various nanostructures as probe tips such as carbon nanotubes and nanowires (NW).

Carbon nanotube probes are typically attached to standard silicon-based cantilevers and are not grown. They are used for force applications in atomic force microscopy (AFM) and electrochemical microscopy [1]–[3]. NWs have been shown to be desirable for unique and advanced scanning probe techniques due to their high-aspect ratio design and robustness. GaAs/AlGaAsIn probes have been grown by molecular beam epitaxy (MBE) but are not used for microwave applications. The metallic NW probes discussed in [4] are used for thermal imaging in Wollastone V shape configuration. Gallium nitride (GaN) NWs have been implemented in scanning probe lithography and scanning tunneling microscopy (STM) [5] as well as scanning microwave impedance microscopy (sMIM) [6].

Manuscript received 17 November 2021; revised 11 March 2022; accepted 19 April 2022. Date of publication 13 May 2022; date of current version 2 August 2022. This work was supported in part by the National Institute of Standards and Technology and in part by the Graduate Fellowships for STEM Diversity. Subject Editor T. Tsuchiya. *(Corresponding author: Kristen L. Genter.)*

Kristen L. Genter is with the National Institute of Standards and Technology, Boulder, CO 80305 USA, and also with the Department of Mechanical Engineering, University of Colorado Boulder, Boulder, CO 80309 USA (e-mail: kristengenter@gmail.com).

Matt D. Brubaker, Samuel Berweger, Kris A. Bertness, and Pavel Kabos are with the National Institute of Standards and Technology, Boulder, CO 80305 USA.

Jonas C. Gertsch and Victor M. Bright are with the University of Colorado Boulder, Boulder, CO 80309 USA.

Color versions of one or more figures in this article are available at https://doi.org/10.1109/JMEMS.2022.3172645.

Digital Object Identifier 10.1109/JMEMS.2022.3172645

The need for non-destructive techniques to evaluate micro- and nano- scale properties makes sMIM a desirable method for a range of materials [7]–[12]. Unlike the previous probes mentioned, these probes can be used for RF applications and allow access to the light-emitting capabilities of direct bandgap III-V semiconductors. These RF measurements enable simultaneous mapping of topography, conductivity, and permittivity.

Tungsten (W)-coated probes have shown significantly enhanced contrast over Al-coated probes for scanned microwave measurements [6]. For this reason, the GaN NWs are coated in W via atomic layer deposition (ALD) creating a microwave pathway from the AFM cantilever body to the GaN NW probe tip. This ALD coating not only improves the capacitive resolution over an order of magnitude, it also does not increase the tip diameter as much as a tip coated in metal via sputtering or evaporation [6]. It has been previously demonstrated that these ALD-coated GaN NWs provide comparable microwave sensitivities to commercial platinum tips as well as an increased lifespan due to their robustness [4]. In these previous studies, the GaN NW probes were fabricated by focused ion beam (FIB) lift-out of individual NWs for pick-and-place transfer and Pt welding onto a traditional AFM tip. In this work, we expand upon previous results to fabricate ALD-coated GaN NWs for sMIM by directly integrating the NW growth into the entire cantilever fabrication process. By doing so, we are able to streamline fabrication of these cantilever devices demonstrating potential for batch production and reduced costs.

### II. Fabrication

We start with a three-inch silicon-on-insulator wafer with a 2 $\mu m$ thick Si <111> device. The GaN NWs are then grown by N-polar selective area epitaxy on GaN/AlN buffer layers coated with a patterned silicon nitride growth mask, as demonstrated with MBE in previous work [13], [14]. Post NW growth, the NWs are protected throughout the AFM cantilever and chip body fabrication process by a 9 $\mu m$ thick polymer photoresist. The thickness is precisely controlled via the amount of photoresist deposited as well as the rotation speed of the wafer.

While protecting both the NW and cantilever area, the silicon nitride growth mask and GaN/AlN buffer layer are etched away using reactive ion etching. Deep-reactive ion etching (DRIE) is then used to etch the device layer to create the cantilevers and their chip bodies. This is followed by another round of DRIE on the handle layer to form the main part of the chip bodies. Hydrofluoric vapor is then used to etch away the buried oxide layer, fully releasing 40 cantilever bodies and creating suspended cantilevers with grown GaN NW probes. The fabrication process up until this point is illustrated in Figure 1.

Lastly, the entire device is put into a viscous flow stainless steel ALD reactor and coated in 3.5 $nm$ $Al_2O_3$/27.9 $nm$ W/1.2 $nm$ $Al_2O_3$ [15], [16]. A witness chip is then measured using X-ray

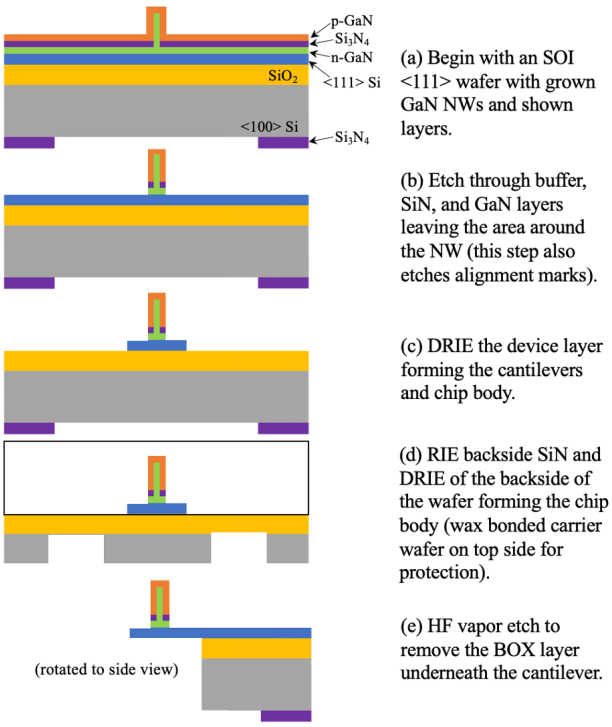


Fig. 1. Simplified schematic of the fabrication process of the GaN NW probes prior to W-ALD coating. This schematic is not to scale.

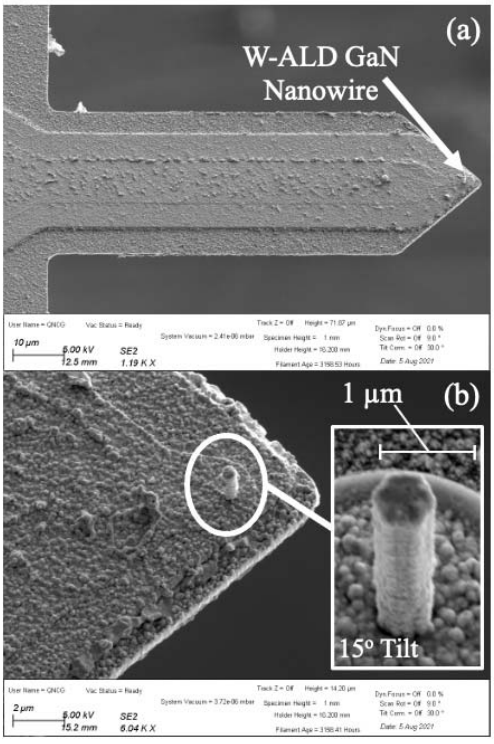


Fig. 2. Finished device: (a) cantilever and (b) selectively grown GaN NW coated in W-ALD.

reflectivity (XRR) to determine the precise thicknesses of the deposited layers. The final device is shown in Figure 2. The resulting W-ALD GaN NWs are approximately 5 $\mu m$ long with a 500 $nm$ diameter.

The stresses in the films on the 2 $\mu m$ device layer initially result in bending of the cantilevers upon release (see Figure 3 a),

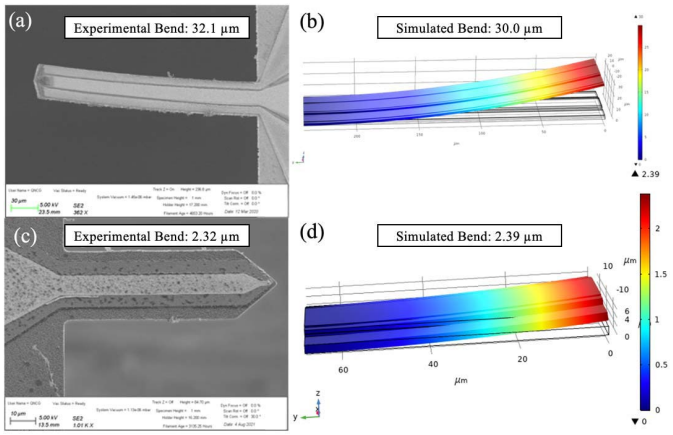


Fig. 3. Experimental vs simulated results of cantilever bend with buffer layer and GaN on 2 $\mu m$ thick silicon. Simulated results were done in COMSOL Multiphysics 5.5.

so measurements and simulations are done to mitigate this effect. The residual stresses of the buffer layer and GaN are obtained through wafer curvature measurements in k-Space MOS Stress Measurement System [17]. Fixed-free 2 $\mu m$ thick silicon cantilevers of various lengths and widths are simulated in COMSOL Multiphysics 5.5 using the residual stresses and thicknesses to determine the optimal dimensions for cantilevers with the least amount of bend [17]. Initial simulations determine the accuracy of the model by comparing it to previously bent cantilevers with SiN mask and GaN/AlN buffer layer on a 2 $\mu m$ silicon device layer. Figure 3b shows these simulated results. The experimental bend and simulated bend are within 7% of each other. This discrepancy could be due to a variety of factors such as the natural tapering of the DRIE etch causing the fabricated cantilever to be narrower or different conditions during the buffer layer and GaN growth causing slight variations in their stresses from what was measured.

Using this model, we are able to design a cantilever with little bending yet still with sufficient length to function in our AFM system. The finished cantilever bend and simulated bend are shown in Figure 3c and d respectively showing less than 7% difference between the two results.

## III. Experimental Method

The setup used is a modified version [18] of the setup previously used for GaN NW cantilevers [6]. The RF signal at 8 GHz is sourced from a network analyzer and sent to the tip through a coaxial resonator. The reflected signal from the resonator is detected using an external in-phase/quadrature (IQ) mixer. This is further expanded upon in [19], [20].

The sample we used to test the RF signals of the newly developed probes involves parallel gold (Au) strips embedded in $SiO_2$. This sample tests the probes in contact mode and in tapping mode while taking topographical and capacitance measurements. A schematic of this sample is shown in Figure 4a. The sample employed for estimates of cantilever sensitivity is a microcapacitor reference sample as seen in [6], [19]. This sample consists of a $SiO_2$ staircase with four $10 \pm 0.3$ $nm$ steps. On each step are four circular pads consisting of 200 $nm$ gold on 20 $nm$ titanium with areas of 0.78, 3.1, 7.1, and 12.6 $\mu m^2$. For sensitivity estimates, only the three smallest circular metal pads on each step are utilized.

## IV. Results

The W-ALD RF cantilevers with selectively grown NWs are first scanned across the sample seen in Figure 4a in contact mode and

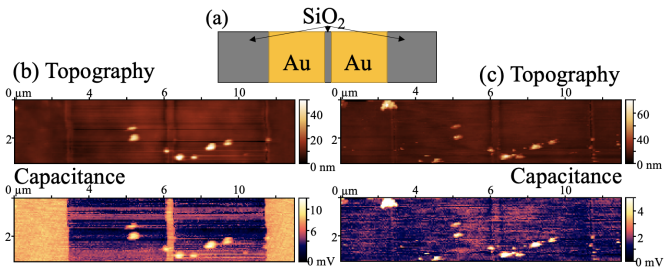


Fig. 4. (a) Schematic of alternating Au and $SiO_2$ sample for topographical and capacitance measurements in (b) contact mode and (c) tapping mode.

then in tapping mode. The results, shown in Figure 4b and c, display the repeatability of the topographical measurements in both modes. In addition, the results show comparable topographical results between the two modes over the same area of the sample. For the capacitance results, the contact mode provides a more sensitive measurement with clear boundaries between the conductive Au and insulative oxide. This boundary is not as distinct in tapping mode due to its intermittent contact with the surface.

The probes are then scanned in contact mode over the reference sample. Utilizing the measured capacitance signal of the smallest capacitor with the thickest oxide, the sensitivity of the probe is determined in a method similar to that in [6]. With a known capacitance of 250 $aF$ [19] and a measured maximum contrast of 20 $mV$ we obtain a conversion of 12.5 $aF/mV$. Together with the RMS noise floor of 1 $mV$, we can estimate a sensitivity limit of $\sim$12.5 $aF$. The obtained results are comparable to those found in [6].

## V. Conclusion

In this work, we develop the first directly grown GaN NW coated in W-ALD for RF and topographical scanning probe measurements. Scanning over various samples, we demonstrate the repeatability of these measurements and estimate a noise-limited sensitivity of 12.5 $aF$. Future improvements include further limiting the bend of the cantilever to provide better topographical measurements when rastered across a staircase sample and minimizing the possible bending of the cantilever in contact mode. In addition, the sensitivity will be improved with a microwave strip line for a more direct pathway for the RF signal.

## References

[1] S. M. Anlage *et al.*, "Scanning probe microscopy: Electrical and electromechanical phenomena at the nanoscale," in *Principles of Near-Field Microwave Micoscopy*, S. V. Kalinin and A. Guverman, Eds. New York, NY, USA: Springer, 2006, pp. 207–245.

[2] J. H. Hafner *et al.*, "Growth of nanotubes for probe microscopy tips," *Nature*, vol. 398, pp. 761–762, Apr. 1999.

[3] H. Dai *et al.*, "Nanotubes as nanoprobes in scanning probe microscopy," *Nature*, vol. 384, pp. 147–150, Nov. 1996.

[4] J. C. Weber *et al.*, "Gallium nitride nanowire probe for near-field scanning microwave microscopy," *Appl. Phys. Lett.*, vol. 104, no. 2, Jan. 2014, Art. no. 023113.

[5] M. Behzadirad *et al.*, "Advanced scanning probe nanolithography using GaN nanowires," *Nano Lett.*, vol. 21, no. 13, pp. 5493–5499, 2021.

[6] J. C. Weber *et al.*, "GaN nanowire coated with atomic layer deposition of tungsten: A probe for near-field scanning microwave microscopy," *Nanotechnology*, vol. 25, no. 41, Oct. 2014, Art. no. 415502.

[7] C. Gao and X.-D. Xiang, "Quantitative microwave near-field microscopy of dielectric properties," *Rev. Sci. Instrum.*, vol. 69, no. 11, pp. 3846–3851, Nov. 1998.

[8] L. Zhang, Y. Ju, A. Hosoi, and A. Fujimoto, "Microwave atomic force microscopy imaging for nanometer-scale electrical property characterization," *Rev. Sci. Instrum.*, vol. 81, no. 12, Dec. 2010, Art. no. 123708.

[9] M. Farina *et al.*, "Calibration protocol for broadband near-field microwave microscopy," *IEEE Trans. Microw. Theory Techn.*, vol. 59, no. 10, pp. 2769–2776, Aug. 2011.

[10] A. Tselev *et al.*, "Near-field microwave scanning probe imaging of conductivity inhomogeneities in CVD graphene," *Nanotechnology*, vol. 23, no. 38, Sep. 2012, Art. no. 385706.

[11] L. T. Hung, N. N. Phuoc, X.-C. Wang, and C. K. Ong, "Temperature dependence dynamical permeability characterization of magnetic thin film using near-field microwave microscopy," *Rev. Sci. Instrum.*, vol. 82, no. 8, Aug. 2011, Art. no. 084701.

[12] C. Plassard *et al.*, "Detection of defects buried in metallic samples by scanning microwave microscopy," *Phys. Rev. B, Condens. Matter*, vol. 83, no. 12, Mar. 2011, Art. no. 121409.

[13] M. D. Brubaker *et al.*, "Polarity-controlled GaN/AlN nucleation layers for selective-area growth of GaN nanowire arrays on Si(111) substrates by molecular beam epitaxy," *Cryst. Growth Des.*, vol. 16, no. 2, pp. 596–604, 2016, doi: 10.1021/acs.cgd.5b00910.

[14] M. D. Brubaker *et al.*, "UV LEDs based on p–i–n core–shell AlGaN/GaN nanowire heterostructures grown by N-polar selective area epitaxy," *Nanotechnology*, vol. 30, no. 23, Jun. 2019, Art. no. 234001.

[15] J. C. Gertsch *et al.*, "$SF_4$ as the fluorination reactant for $Al_2O_3$ and $VO_2$ thermal atomic layer etching," *Chem. Mater.*, vol. 31, pp. 3624–3635, Apr. 2019.

[16] S. M. George, "Atomic layer deposition: An overview," *Chem. Rev.*, vol. 110, no. 1, pp. 111–131, 2010.

[17] *Certain Commercial Equipment, Instruments or Materials are Identified to Adequately Specify the Experimental Procedure. Such Identification Does not Imply Recommendation or Endorsement by the National Institute of Standards and Technology, nor Does it Imply that the Materials or Equipment Identified are Necessarily the Best Available for the Purpose*, NIST, Boulder, CO, USA, 2021.

[18] S. Berweger *et al.*, "Imaging carrier inhomogeneities in ambipolar tellurene field effect transistors," *Nano Lett.*, vol. 19, no. 2, pp. 1289–1294, 2019.

[19] H. P. Huber *et al.*, "Calibrated nanoscale capacitance measurements using a scanning microwave microscope," *Rev. Sci. Instrum.*, vol. 81, no. 11, Nov. 2010, Art. no. 113701.

[20] A. Imtiaz *et al.*, "Frequency-selective contrast on variably doped p-type silicon with a scanning microwave microscope," *J. Appl. Phys.*, vol. 111, no. 9, May 2012, Art. no. 093727.